

Coriander Leaf Extract Exerts Antioxidant Activity and Protects Against UVB-Induced Photoaging of Skin by Regulation of Procollagen Type I and MMP-1 Expression

Eunson Hwang,¹ Do-Gyeong Lee,² Sin Hee Park,^{3,4} Myung Sook Oh,⁵ and Sun Yeou Kim^{6–8}

¹Department of Oriental Medicinal Material and Processing, College of Life Science, Kyung Hee University, Yongin-Si, Korea.

²Graduate School of Biotechnology, College of Life Science, Kyung Hee University, Yongin-Si, Korea.

³Graduated School of East-West Medical Science, Kyung Hee University, Yongin-Si, Korea.

⁴Gyeonggi Institute of Health & Environment, Suwon, Korea.

⁵Department of Life and Nanopharmaceutical Science, Kyung Hee East-West Pharmaceutical Research Institute, Kyung Hee University, Seoul, South Korea.

⁶Gachon Institute of Pharmaceutical Science, Gachon University, Incheon, Korea.

⁷College of Pharmacy, Gachon University, Incheon, Korea.

⁸Gachon Medical Research Institute, Gil Medical Center, Incheon, Korea.

ABSTRACT Ultraviolet (UV) radiation causes photodamage to the skin, which, in turn, leads to depletion of the dermal extracellular matrix and chronic alterations in skin structure. Skin wrinkles are associated with collagen synthesis and matrix metalloproteinase-1 (MMP-1) activity. *Coriandrum sativum* L. (coriander leaf, cilantro; CS) has been used as a herbal medicine for the treatment of diabetes, hyperlipidemia, liver disease, and cancer. In this study, we examined whether CS ethanol extract (CSE) has protective effects against UVB-induced skin photoaging in normal human dermal fibroblasts (NHDF) *in vitro* and in the skin of hairless mice *in vivo*. The main component of CSE, linolenic acid, was determined by gas chromatography-mass spectroscopy. We measured the cellular levels of procollagen type I and MMP-1 using ELISA in NHDF cells after UVB irradiation. NHDF cells that were treated with CSE after UVB irradiation exhibited higher procollagen type I production and lower levels of MMP-1 than untreated cells. We found that the activity of transcription factor activator protein-1 (AP-1) was also inhibited by CSE treatment. We measured the epidermal thickness, dermal collagen fiber density, and procollagen type I and MMP-1 levels in photo-aged mouse skin *in vivo* using histological staining and western blot analysis. Our results showed that CSE-treated mice had thinner epidermal layers and denser dermal collagen fibers than untreated mice. On a molecular level, it was further confirmed that CSE-treated mice had lower MMP-1 levels and higher procollagen type I levels than untreated mice. Our results support the potential of *C. sativum* L. to prevent skin photoaging.

KEY WORDS: • *Coriandrum sativum* • hairless mice • MMP-1 • procollagen type I • UVB

INTRODUCTION

CORIANDRUM SATIVUM L. (CS), commonly known as coriander, is an annual herb belonging to the family Apiaceae (Umbelliferae) that has been extensively cultivated for centuries in many temperate climates such as the Middle East, Latin American, Africa, and Asia.¹ Traditionally, both the seeds and aerial parts of coriander are used as food elements. Fresh leaves are used as a flavoring agent, and

dried coriander seeds are used as spices in food preparation.² The main chemical constituents in coriander seeds are essential oils and monoterpenoids, such as linalool. In addition to volatile oils, caffeic acid and flavonoid glycosides have been isolated from CS leaves.³ In this study, we analyzed linolenic acid, which is a main component of CS ethanol extract (CSE) by gas chromatography-mass spectroscopy (GC-MS). Previous studies have found that CS has hypoglycemic, hypolipidemic, hepatoprotective, antimutagenic, antihypertensive, and antifertility effects.^{4–9} Dermatological effects of CS include anti-inflammatory activity in erythema induced by ultraviolet (UV) light and antioxidant effects.^{10–12} However, the protective effects of CS against UV-induced photoaging of the skin have not been reported.

Manuscript received 26 July 2013. Revision accepted 28 April 2014.

Address correspondence to: Sun Yeou Kim, PhD, College of Pharmacy, Gachon University, 191 Hambakmoero, Yeonsu-Gu, Incheon 406-799, Republic of Korea, E-mail: sunykim@gachon.ac.kr

UV radiation, in particular UVB (290–320 nm) from sunlight, is one of the most important environmental factors that damage the skin. Premature aging of the skin, called photoaging, is caused by repetitive exposure to solar radiation. Photoaging that results in the degradation of extracellular matrix (ECM) proteins, including type I collagen, elastin, proteoglycans, and fibronectin, is characterized by coarse wrinkles, thickness, roughness, mottled pigmentation, and histologic changes.^{13,14} Disorganization, fragmentation, and dispersion of collagen bundles are other prominent features of photodamaged human skin.¹⁵

The matrix metalloproteinases (MMPs) are a family of structurally related matrix-degrading enzymes that play important roles in various destructive processes, including inflammation, tumor invasion, and skin aging.¹⁶ In particular, MMP-1, known as interstitial collagenase, initiates the degradation of collagen types I, II, and III in the skin.¹⁷ Type I collagen is synthesized as procollagen type I, a soluble precursor secreted by fibroblasts when organizing the main ECM components.¹⁸ Upregulation of UV-induced MMPs in dermal fibroblasts leads to the breakdown of collagen and other ECM proteins.¹⁹ The MMP promoter contains an activator protein-1 (AP-1) binding site, and UV-induced activation of AP-1 has been shown to increase MMP-1 expression.²⁰ UV-inducible transcription factor AP-1 complexes consist of Jun and Fos family members.²¹

Skin photoaging is also related to reactive oxygen species (ROS) generated by sun exposure.²² Long-term exposure to sunlight and short-term overexposure overwhelm biological antioxidant systems, which scavenge ROS such as free radicals.²³ Furthermore, it has been found that the accumulation of ROS plays a critical role in the photoaging of human skin, resulting in the upregulation of MMP-1 and the degradation of dermal collagen.²⁴ Accordingly, we wanted to investigate the antioxidant effects of CSE.

The aim of this study was to examine the effects of CSE against UVB-induced skin photoaging in normal human dermal fibroblasts (NHDFs) *in vitro* and in the skin of hairless mice *in vivo*. To the best of our knowledge, this study is the first to research the effects of *C. sativum* (CSE) on skin photoaging.

MATERIALS AND METHODS

Chemicals

Dulbecco's modified Eagle's medium (DMEM), fetal bovine serum (FBS), and penicillin streptomycin were purchased from Gibco BRL (Grand Island, NY, USA). 3-(4,5-Dimethylthiazol-2-yl)-2,5-diphenyltetrazolium bromide (MTT), dimethylsulfoxide (DMSO), and a Masson's trichrome stain kit were purchased from Sigma-Aldrich (St. Louis, MO, USA). Antibodies against type I procollagen, MMP-1, and α -tubulin were purchased from Santa Cruz Biotechnology (Santa Cruz, CA, USA). The ELISA kit for procollagen type I was obtained from Takara (Procollagen Type I C-Peptide EIA Kit; Takara, Shiga, Japan). ELISA kits for MMP-1 were purchased from R&D Systems (Human Total MMP-1 kit; R&D Systems, Inc., Minneapolis, MN, USA).

Preparation of the CS extracts and standardization

The CS was extracted as previously described.²⁵ In addition, the fatty acid composition of CSE has been analyzed and previously characterized by our research group.²⁵ Fresh CS was purchased from a local market (Incheon, Korea), and a voucher specimen (KHUOPS-CMH002) was deposited in the herbarium at the College of Pharmacy at Kyung Hee University (Seoul, Korea). First, 500 g of CS leaves were mixed with 5 L of 70% ethanol in a blender at high speed for 5 min. Then, the extract was filtered, evaporated on a rotary vacuum evaporator, and lyophilized (yield 4.00%). The powder (CSE) was stored at 4°C before use.

Quantitative analysis of linolenic acid from CSE by GC-MS

The exact amount of linolenic acid was dissolved in chloroform (CHCl₃), and diluted to an appropriate concentration. The solution of standard at 1 mg/mL was prepared. A set of standard solutions was prepared by diluting the stock solution with CHCl₃ to concentrations ranging from 0.1 to 100 ppm. For more sensitive and less contaminable analysis, H₂O fraction of CSE was removed by partition using EtOAc, BuOH, and H₂O. The sample solution was prepared by adding 1 mL of CHCl₃ on 1.5 mg of EtOAc fraction and injected onto the GC-MS for the quantitative determination of linolenic acid. GC-MS was performed on a Shimadzu 2010 gas chromatograph interfaced with a single-quadrupole QP2010 plus (Shimadzu, Tokyo, Japan). The electron energy was 70 eV, and ion source temperature was 250°C. Sample solutions (1 μ L) were injected into the GC with a 10:1 split ratio at 280°C and separated through a DB-5 column (0.25 μ m film thickness \times 0.53 mm diameter \times 30 m length). The oven temperature was programmed as follows: 60°C for 2 min, increased to 320°C at a rate of 15°C, and held for 10 min. Helium was used as the carrier gas at a flow of 14.9 mL/min. Peak identification was achieved by comparing the retention time and matching the high ratio of the characteristic ions.

Cell culture

NHDFs were obtained by skin biopsy from a healthy young male donor (MCTT Core, Inc., Seoul, Korea). The cells were plated in 100-mm tissue culture dishes and cultured in DMEM supplemented with 10% heat-inactivated FBS and 1% penicillin–streptomycin at 37°C in a humidified atmosphere containing 5% CO₂. All experiments were performed using only cells between passages 6 and 10.

UVB irradiation and CSE treatment

UVB irradiation and sample treatment were performed according to the method previously reported by Hwang *et al.*²⁶ NHDFs were seeded in 40-mm tissue culture dishes (1.2 \times 10⁵ cells). When cells reached more than 80% confluence, they were rinsed twice with phosphate-buffered saline (PBS) and all irradiations were performed under a thin layer of PBS. The plate was closed during irradiation. UVB radiation was supplied by a closely spaced array of

five Sankyo Denki sunlamps, which delivered uniform radiation at a distance of 7.5 cm. The irradiance (0.1 mW/cm^2) was measured using a UVB photometer (IL1700 photometer; International Light, Peabody, MA, USA). The cells were irradiated with UVB (144 mJ/cm^2) for 40 sec. Immediately after irradiation, the cells were washed thrice with warm PBS, after which $1980 \mu\text{L}$ of fresh serum-free medium and $20 \mu\text{L}$ of sample were added to each well for the indicated time. Control cells were kept in the same culture conditions without UVB exposure. AP-1 activation was determined in cells harvested at 4 h after UVB irradiation. Procollagen type I expression and MMP-1 secretion were assessed in the supernatants harvested at 72 h after UVB irradiation. For measurement of ROS production, cells were harvested at 24 h after UVB irradiation.

Measurement of ROS production

After 24 h of UVB irradiation (144 mJ/cm^2) and sample treatment, NHDFs were stained with $30 \mu\text{M}$ 2',7'-dichlorofluorescein diacetate (DCFH-DA; Sigma-Aldrich) for 30 min at 37°C in a CO_2 incubator. The cells were then analyzed by flow cytometry (FACSCalibur™; Becton-Dickinson, San Jose, CA, USA).

Measurement of procollagen type I and MMP-1

The concentrations of procollagen type I and MMP-1 in the medium were determined using commercially available ELISA kits (Procollagen Type I C-Peptide EIA Kit, Takara; Human Total MMP-1 kit, R&D Systems, Inc.) according to the manufacturer's instructions. Each sample was analyzed in triplicate.

MTT assay

The MTT assay is a colorimetric assay used to measure cell viability (CV) that reduces MTT to formazan dyes, producing a purple color. After 72 h of incubation, the volume of the medium was decreased to 1 mL and $100 \mu\text{L}$ of 1 mg/mL MTT was added to each well. Next, the cells were incubated in the presence of 5% CO_2 and 95% O_2 at 37°C for 2 h. The substrate-containing medium was carefully removed by a suction pump designed for in cell culture (Welch 2515C-75; Gardner Denver Product, Quincy, IL, USA), and 1 mL of DMSO was added to each well to dissolve the formazan crystals. The plates were shaken on an orbital shaker (SH30; FINEPCR Co., Seoul, Korea) for 30 min at room temperature. The absorbance of $100 \mu\text{L}$ aliquots was quantified by measuring the optical density (OD) at 570 nm using a microplate reader (E09090; Molecular Devices, San Francisco, CA, USA). Blank group means cells and sample-free condition; it was measured by using a spectrophotometer. CV for a well was calculated by the equation: $\text{CV} = (\text{the OD value of treated well} / \text{the OD value of nontreated control well}) \times 100\%$.²⁷

Animals

We purchased 6-week-old male Hos:HR-1 hairless mice (20–27 g; $n=25$) from Central Lab Animals, Inc. (Seoul,

Korea). The mice were housed in a temperature- and humidity-controlled room ($22^\circ\text{C} \pm 1^\circ\text{C}$, $60\% \pm 5\%$ humidity) with a 12 h light/12 h darkness cycle. The mice were adapted to their surroundings at least 3 days before beginning the experiments. During the experimental period, the mice were allowed free access to food and water. We randomly divided the 25 hairless mice into 5 groups of 5 mice per cage: (i) no UVB exposure (control group), (ii) UVB irradiation alone, (iii) UVB irradiation with 0.5% CSE treatment, (iv) UVB irradiation with 1% CSE treatment, and (v) UVB irradiation with 1% retinyl palmitate (RP) treatment. RP was used as a positive control. The experimental protocol [KHUASP-11-05] was approved by the Institutional Animal Care and Use Committee of Kyung Hee University.

Measurement of wrinkles induced by UVB irradiation

UVB radiation was applied to the dorsal skin of the mice. The mice were exposed to UVB radiation seven times per week at 100 mJ/cm^2 (1 min 10 sec) for the first week (1 minimal erythema dose = 100 mJ/cm^2),²⁸ then at 200 mJ/cm^2 (2 min 21 sec) thrice a week for 2 weeks, and finally to 400 mJ/cm^2 (4 min 43 sec) twice a week for 2 weeks (total dose of 3500 mJ/cm^2). After 1 week of UVB irradiation alone, mice were treated with CSE or RP thrice a week for 4 weeks. We applied $400 \mu\text{L}$ of solution containing 0.5% CSE, 1% CSE, and 1% RP dissolved in propanediol/ethanol (7:3) with a brush to the dorsal skin of the mice. The wrinkles on the backs of the mice were photographed using a digital camera before they were sacrificed. This is a modification of the method described by Chiu *et al.*²⁹ and Cho *et al.*³⁰

Histological analysis

The mice were sacrificed after the final UVB exposure and sample treatment, and biopsies were obtained from the dorsal skin. The biopsies were fixed in 4% paraformaldehyde for 24 h and embedded in paraffin. Sections $\sim 4 \mu\text{m}$ thick were stained with hematoxylin for 10 min, washed, and stained with eosin for 2 min. After washing with water, the slides were gradually dehydrated in 50%, 70%, 90%, and 100% ethanol. Other samples were stained with Masson's trichrome to examine collagen density in the dermis. These sections were stained first with Bouin solution at 56°C for 1 h, then washed, and stained with Weigert's iron hematoxylin working solution for 10 min. Slides were subsequently washed and differentiated in phosphomolybdic-phosphotungstic acid solution for 10–15 min, and then stained with aniline blue solution for 5–10 min. After washing, the slides were quickly dehydrated using 95% and 100% ethanol. The stained slides were examined with a light microscope.

Western blot analysis

Western blots were performed using total cell and tissue lysates. After treatment, cells were harvested and washed in PBS. Cell and tissue samples were homogenized with lysis

buffer containing 50 mM Tris-Cl, pH 8.0, 0.1% sodium dodecyl sulfate (SDS), 150 mM NaCl, 1% NP-40, 0.02% sodium azide, 0.5% sodium deoxycholate, 100 $\mu\text{g}/\text{mL}$ PMSF, 1 $\mu\text{g}/\text{mL}$ aprotinin, and a phosphatase inhibitor. The lysates were then subjected to centrifugation at 12,000 g for 20 min. All reactions were performed in triplicate. Protein concentrations were measured using Bradford reagent (Bio-Rad, Hercules, CA, USA) with bovine serum albumin as the standard. The skin cell and tissue lysates containing equal amounts of total protein were separated by 8% or 10% SDS-polyacrylamide gel electrophoresis and then transferred to a nitrocellulose membrane (Amersham Pharmacia Biotech, Buckinghamshire, United Kingdom). Next, the membrane was blocked with a solution containing 5% nonfat milk in TBST for 1 h at room temperature and then incubated overnight with primary antibody at 4°C. The membranes were washed thrice with TBST and incubated with secondary antibodies (Santa Cruz Biotechnology, Inc.) for 1 h at room temperature. Finally, the immune complexes were detected with an ECL western blot detection system (LAS-4000; Fujifilm, Tokyo, Japan). Densitometry analysis of bands was performed with ImageMaster™ 2D Elite soft-

ware, version 3.1 (Amersham Pharmacia Biotech, Piscataway, NJ, USA).

Statistical analysis

All experiments were carried out in triplicate. The data are expressed as means \pm SD. A statistical comparison between different treatments was performed using a one-way analysis of variance followed by Duncan's test, and then Student's *t*-test was used to compare individual treatments with the controls. Statistical significance was set at $P < .05$.

RESULTS

Quantitative analysis of linolenic acid from CSE

Our group had already reported results of the analysis of the fatty acid composition of coriander leaves. The concentration of total fatty acids in CSE was 4.71/100 g.²⁵ In this study, linolenic acid, the main component from CSE, was quantified by GC-MS. The retention time of the linolenic acid, as a standard compound, was 15.41 min (Fig. 1). Linolenic acid from CSE samples was identified by a

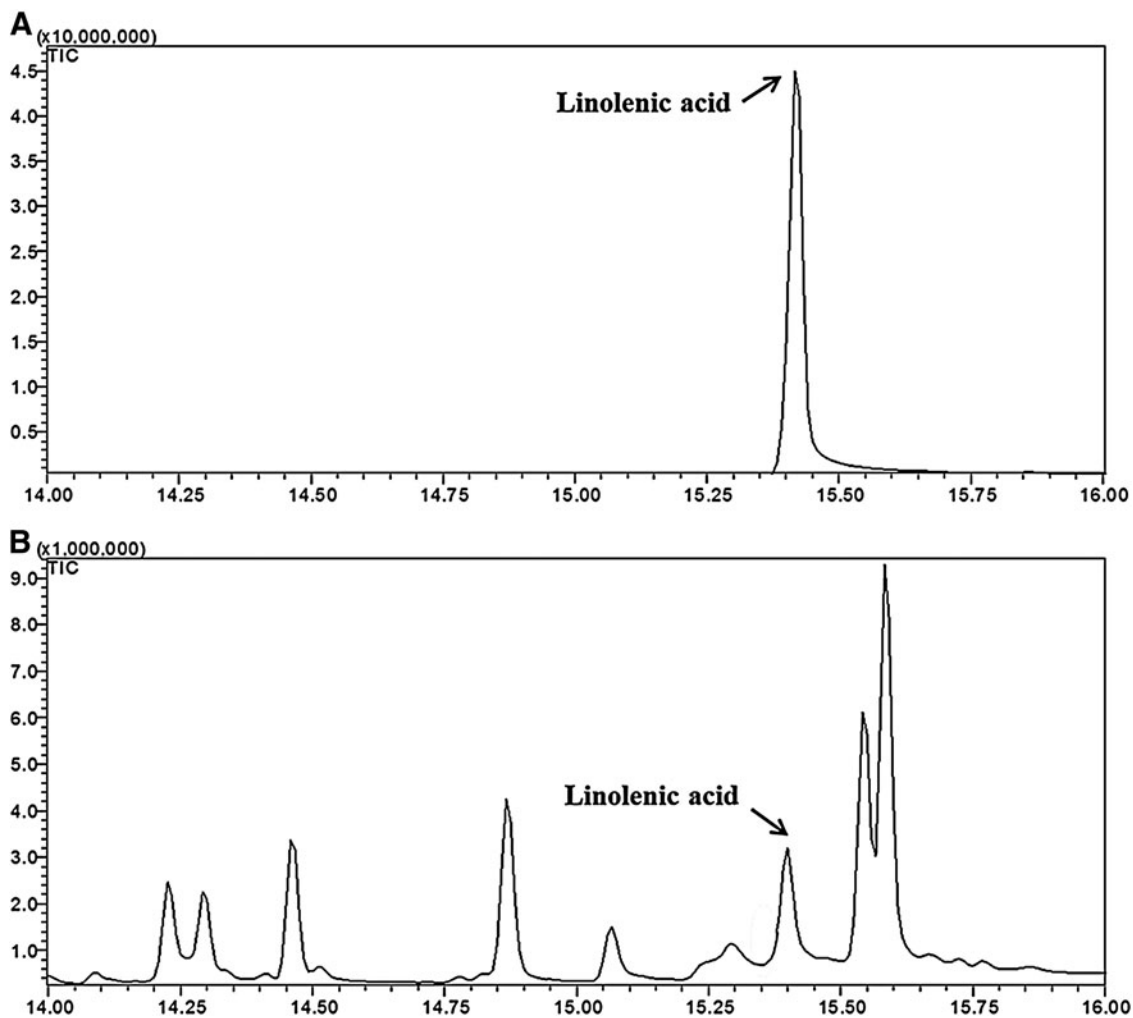


FIG. 1. Chromatogram of linolenic acid standard (100 ppm) (A) and EtOAC fraction of CS ethanol extract (CSE) (1500 ppm) (B).

comparison of retention times with those of the corresponding standards. The linolenic acid calibration curve was linear with a correlation coefficient of 1.0000. The content of linolenic acid from CSE was 0.020 ± 0.0006 mg/mg.

Effects of CSE on intracellular ROS production in UVB-irradiated NHDFs

NHDFs have been used to investigate UVB-induced production of ROS using FACS analysis. As shown in Figure 2, UVB-irradiated cells noticeably increased ROS generation compared with nonirradiated cells. CSE treatment at a concentration of $100 \mu\text{g/mL}$ led to a 43% decline in ROS level compared with the UVB-irradiated control cells.

Procollagen type I expression, MMP-1 secretion, and CV in CSE-treated cultured human dermal fibroblasts

The effects of CSE on procollagen type I expression and MMP-1 secretion were studied in cultured human dermal fibroblasts that were not exposed to UVB. Nonirradiated control cells were considered 100% viable. At concentrations ranging from 1 to $100 \mu\text{g/mL}$, CSE had no significant cytotoxic effects in the human dermal fibroblasts (Fig. 3A). Treatment with CSE at a high concentration ($100 \mu\text{g/mL}$) strongly increased procollagen type I production (up to 50%) compared with normal cells. The effect of CSE on procollagen type I expression was dose dependent (Fig. 3B). MMP-1 secretion was about 20% lower in cells treated with $100 \mu\text{g/mL}$ CSE than in nonirradiated controls (Fig. 3C).

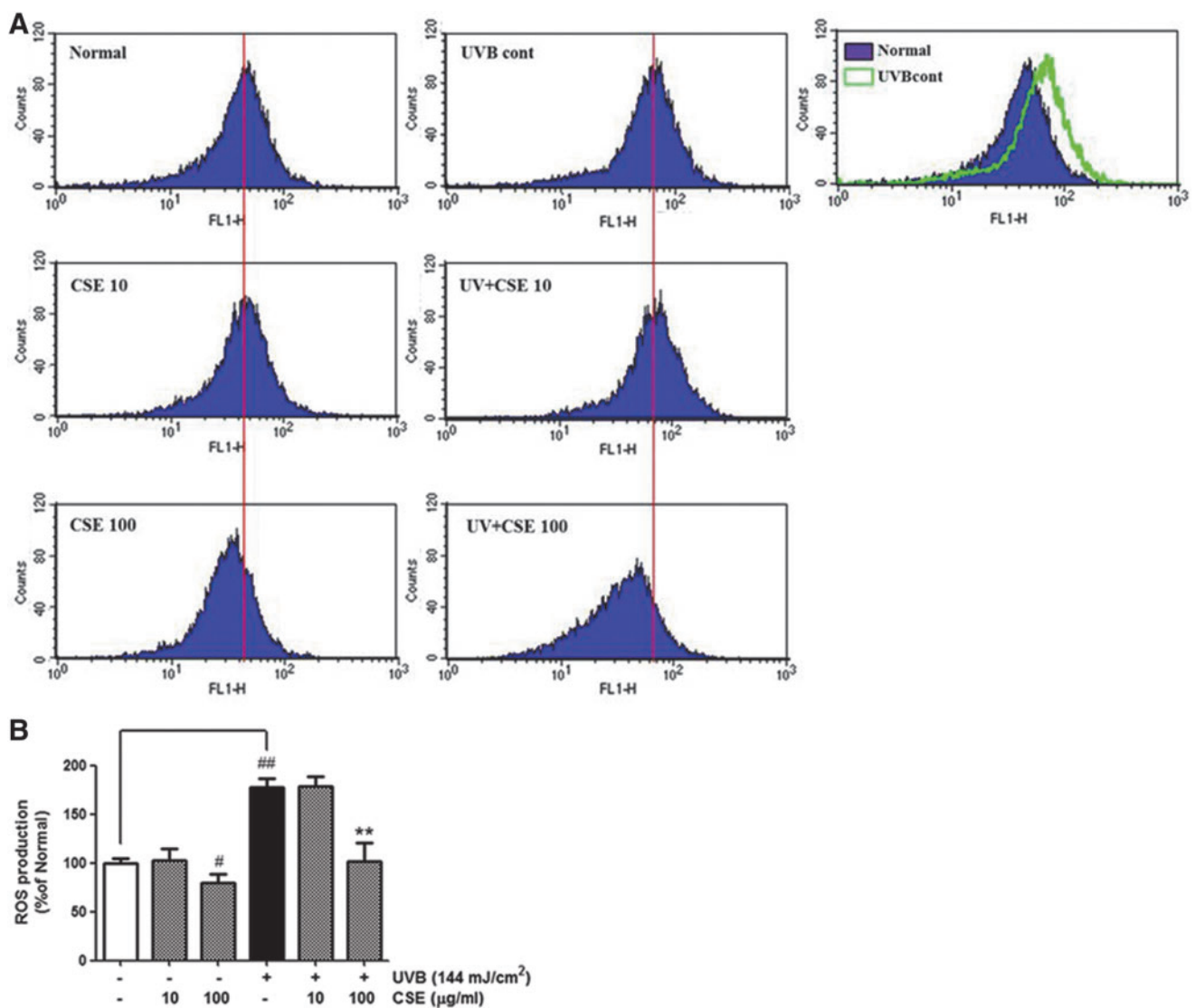


FIG. 2. Levels of reactive oxygen species (ROS) in normal human dermal fibroblasts treated as indicated for 24 h were measured by flow cytometry with the DCFH-DA dye. The number of cells is plotted *versus* the dichlorofluorescein fluorescence detected by the FL-1 channel (A). The relative ROS production of cells is expressed in each histogram (B). Values are means \pm SD. # and * indicate significant differences ($P < .05$) between the ultraviolet (UV) (-) control and UV (+) control, respectively. ## $P < .01$ versus the normal control, * $P < .05$ and ** $P < .01$ versus UVB-irradiated control. Color images available online at www.liebertpub.com/jmf

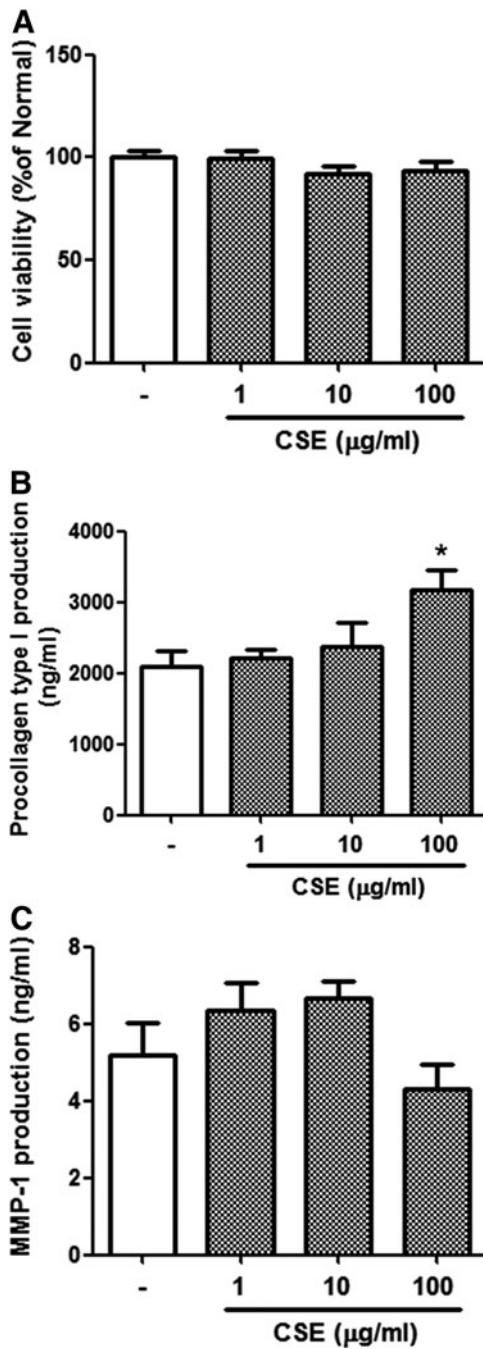


FIG. 3. Cell viability (A), procollagen type I level (B), and matrix metalloproteinase-1 (MMP-1) level (C) in CSE-treated cultured human dermal fibroblasts. Cells were incubated in the absence or presence of CSE at concentrations ranging from 1 to 100 $\mu\text{g/ml}$ for 72 h. Values are means \pm SD. Statistical significance compared with UV (-) control cells; * $P < .5$.

Procollagen type I expression, MMP-1 secretion, and CV in UVB-irradiated and CSE-treated cultured human dermal fibroblasts

We compared the viability of cells treated with UVB (144 mJ/cm^2) alone or UVB (144 mJ/cm^2) plus CSE (1–100 $\mu\text{g/ml}$) using the MTT assay. The resulting survival curve is

shown in Figure 4A. Nonirradiated control cells were considered 100% viable. The viability of cells treated with UVB radiation alone was $\sim 20\%$. The viability of UVB-irradiated cells treated with CSE was also lower than that of the control cells.

To determine the effects of CSE on UV-damaged skin, we examined cellular levels of procollagen type I and MMP-1 secretion. UVB-irradiated fibroblasts had lower procollagen type I expression and higher MMP-1 expression than unexposed cells. We found that cells treated with CSE did not exhibit procollagen type I suppression after UVB exposure. Even treatment with CSE at 100 $\mu\text{g/ml}$ induced greater procollagen type I production (up to 266%) than in

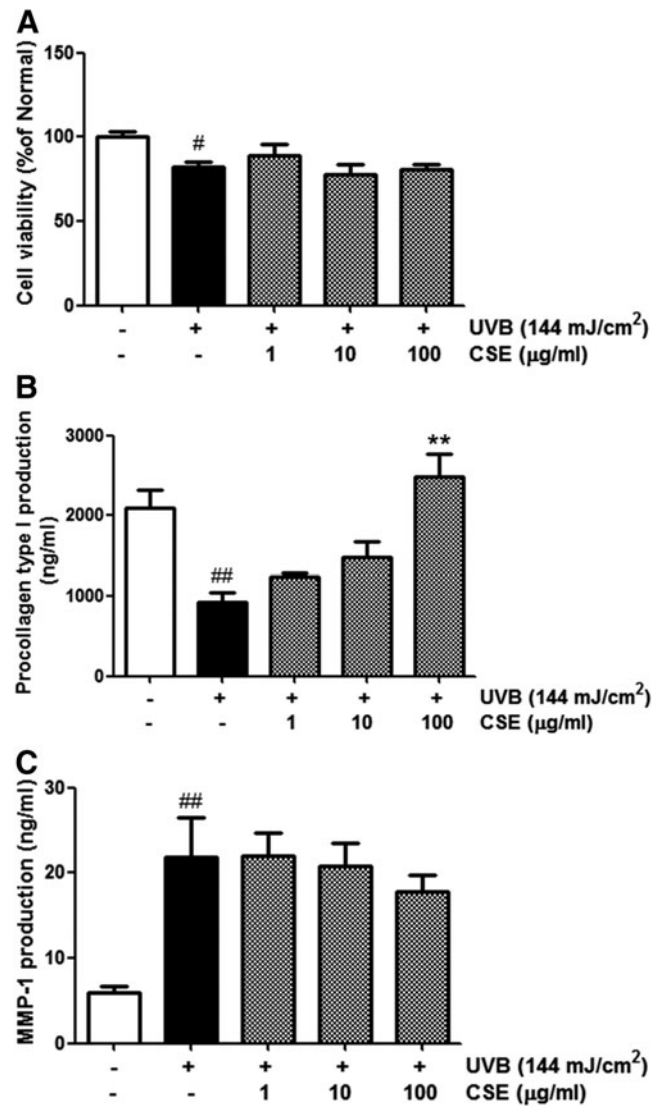


FIG. 4. Cell viability (A), procollagen type I levels (B), and MMP-1 levels (C) in UVB-irradiated and CSE-treated cultured human dermal fibroblasts. Cells were irradiated with UVB (144 mJ/cm^2) and then incubated in the absence or presence of CSE at concentrations ranging from 1 to 100 $\mu\text{g/ml}$ for 72 h. Values are means \pm SD. # and * indicate significant differences ($P < .05$) between the UV (-) control and UV (+) control, respectively. # $P < .05$ and ## $P < .01$ versus the normal control, ** $P < .01$ versus UV-treated control.

UVB-irradiated controls (Fig. 4B). In other words, cells treated with CSE after UVB irradiation produced more procollagen type I than cells that were irradiated and not exposed to CSE. In addition, UVB-irradiated cells treated with 10 and 100 $\mu\text{g}/\text{mL}$ CSE had a 5% and 19% lower MMP-1 expression, respectively, compared with untreated cells (Fig. 4C). Interestingly, the effect of CSE on procollagen type I production and MMP-1 expression was dose dependent. These results provide evidence that CSE prevents the MMP-1 elevation and procollagen type I reduction which are observed after UVB irradiation.

Inhibitory effect of CSE on AP-1 activation

UV-inducible transcription factor AP-1 is composed of c-Jun and c-Fos proteins. To investigate the effects of CSE on UVB-induced AP-1 expression, human dermal fibroblasts were irradiated with UVB at 144 mJ/cm^2 and then treated with CSE for 4 h. The levels of phosphorylated c-Jun and c-Fos were increased in fibroblasts that were UVB irradiated. However, expression of AP-1 was reversed by treatment with CSE (Fig. 5A). Even though the total c-Jun and c-Fos levels were not changed, the activated form of c-Jun (p-c-Jun) and c-Fos (p-c-Fos) expression was markedly lower after treatment with 10 and 100 $\mu\text{g}/\text{mL}$ CSE (Fig. 5B).

Inhibition of UV-induced changes of the dorsal skin by topical CSE treatment

We measured the thickness of dorsal skin in UVB exposed- and -unexposed mice. As shown in Figure 6A, the dorsal skin of UVB-irradiated mice was thicker than that of unexposed mice. The effects of CSE on UVB-irradiated skin

of mice were investigated histochemically. Epidermal thickness and collagen content were evaluated with hematoxylin and eosin staining. Induction of skin photoaging caused significant skin epidermal thickness in UVB-irradiated mice, but treatment with CSE or RP decreased skin epidermal thickness in UVB-irradiated mice (Fig. 6B). In addition, we observed intense staining of collagen by Masson's trichrome. The collagen fibers of UVB-irradiated mice were less dense and more erratically arranged compared with the dense, regular fibers of nonirradiated mice. We also found that accumulation of collagen in the dermis was remarkable in the CSE- or RP-treated group compared with untreated UVB-exposed mice (Fig. 6C). These results suggest that CSE may block UVB-induced alterations of collagen and increase epidermal thickness.

Expression of procollagen type I and MMP-1 proteins in the skin of UVB-irradiated and CSE-treated mice

To study the effects of CSE on UVB-induced procollagen type I and MMP-1 protein expression, western blot analysis was performed on tissue lysates from hairless mice skin. UVB-irradiated mice treated topically with CSE exhibited intensified procollagen type I and attenuated MMP-1 protein levels compared with untreated UVB-irradiated mice (Fig. 7). These results suggest that CSE may inhibit UVB-induced photoaging through the regulation of procollagen type I and MMP-1 expression.

DISCUSSION

The skin's natural antioxidant defenses, which neutralize free radicals, can be overwhelmed by high doses of UV light.

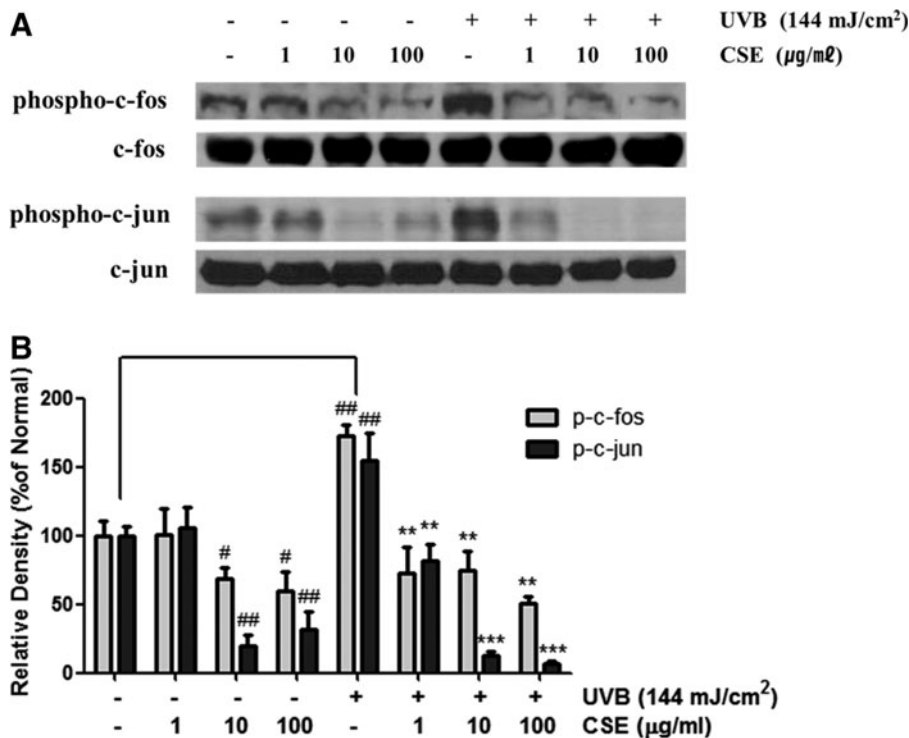


FIG. 5. Effect of CSE on the phosphorylation of c-fos and c-jun (A), and results of densitometric analysis (B) in UVB-irradiated cultured human dermal fibroblasts. Cells were irradiated with UVB (144 mJ/cm^2) and treated with CSE at concentrations ranging from 1 to 100 $\mu\text{g}/\text{mL}$ for 4 h. We performed western blot analysis on 50 μg of total protein from cell lysates. Equal loading was confirmed using anti-c-fos and anti-c-jun antibodies. The densitometry analysis data are expressed as a percentage relative to the UVB-untreated control. Values are means \pm SD. # and * indicate significant differences ($P < .05$) between the UV (-) control and UV (+) control, respectively. # $P < .05$ and ## $P < .01$ versus the normal control, ** $P < .01$ and *** $P < .001$ versus UV-treated control.

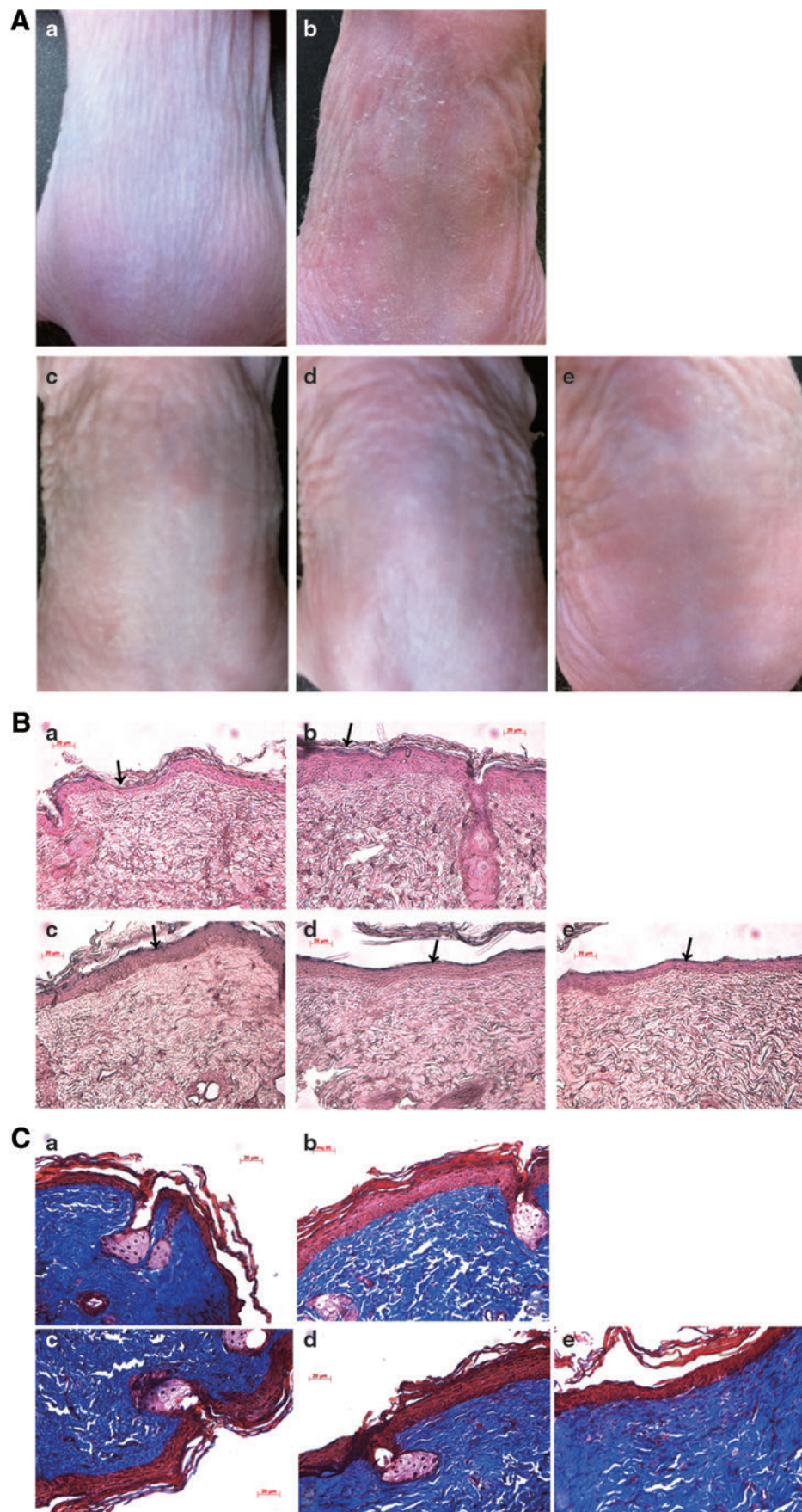


FIG. 6. Representative photographs (A) of hematoxylin and eosin-stained sections (B), and of Masson's trichrome-stained sections (C) from the dorsal skin of hairless mice. After 1 week of UVB irradiation, the CSE treatment was applied topically thrice a week for 4 weeks. The scale bar represents 20 μm . (a) Control group; (b) UVB irradiation group; (c) UVB irradiation with 0.5% CSE; (d) UVB irradiation with 1% CSE; and (e) UVB irradiation with 1% retinyl palmitate (RP). Color images available online at www.liebertpub.com/jmf

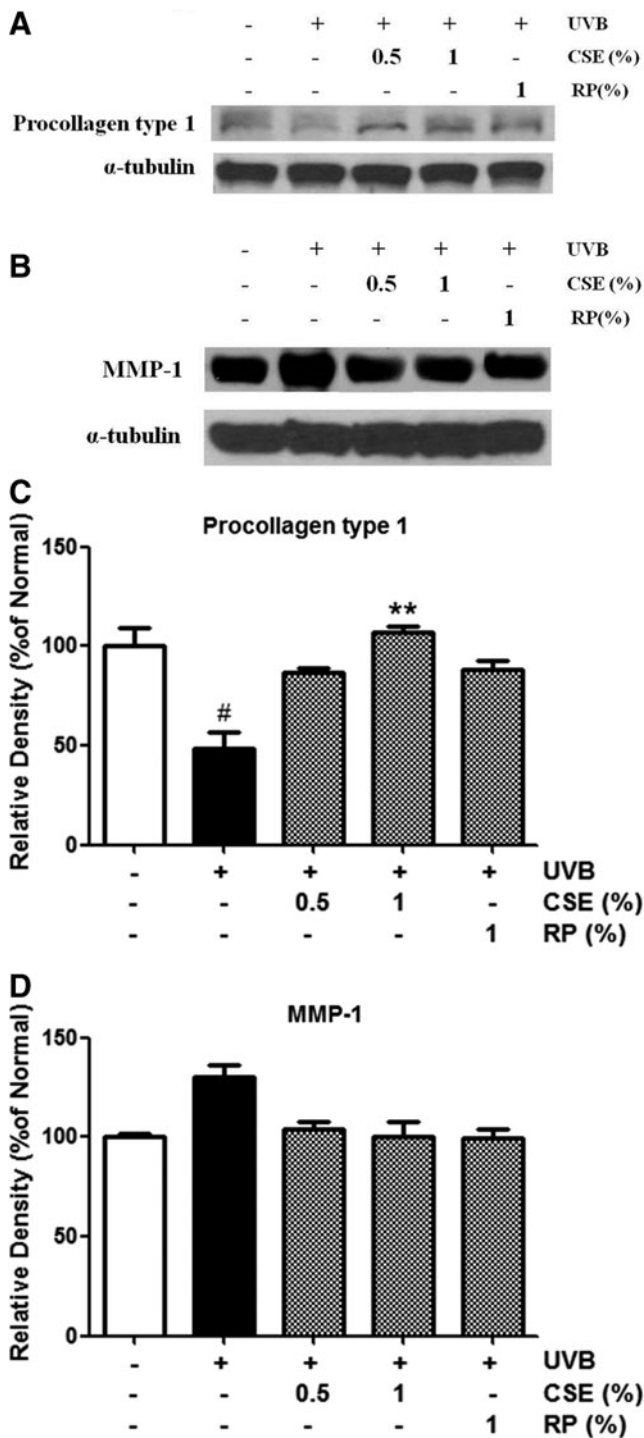


FIG. 7. Protein expressions of procollagen type I (A) and MMP-1 (B). Changes according to densitometric analysis (C,D) in the skin of UVB-irradiated and CSE-treated hairless mice. Mice were irradiated with UVB (400 mJ/cm²), treated with 0.5% and 1% CSE, and treated with 1% RP thrice a week for 4 weeks. We performed western blot analysis on 40 μ g of total protein from skin tissue lysates. Equal loading was confirmed using antibodies to α -tubulin. The densitometry analysis data are expressed as a percentage relative to the UVB-untreated control. Values are means \pm SD. # and * indicate significant differences ($P < .05$) between the UV (-) control and UV (+) control, respectively. ## $P < .01$ versus the normal control, ** $P < .01$ versus UV-treated control.

As a result, cellular components such as proteins, lipids, and DNA can be damaged by free radicals.^{31,32} Therefore, ROS are considered involved in the skin's aging process. It has been previously reported that CS has the ability to scavenge the free radical 2,2-diphenyl-1-picrylhydrazyl (DPPH) and exhibited antioxidant activity superior to ascorbic acid.^{33,34} Recently, Park *et al.* demonstrated the protective effects of CS leaves against oxidative stress in human keratinocytes.²⁵ Therefore, we hypothesized that CSE would have protective effects against oxidative stress in skin fibroblasts. As expected, Figure 2 showed that the cells treated with 100 μ g/mL CSE exhibited suppressed ROS production under both non-irradiated and UVB-irradiated conditions. Oxidative stress may lead to the activation of AP-1, thus increasing MMP expression and collagen degradation.²⁰ In other words, UVB irradiation of NHDFs stimulated ROS production, which leads to activation of AP-1, increased MMP-1 secretion, and decreased procollagen type I production. As shown in Figure 5, CSE markedly lowered phosphorylation of c-Jun and c-Fos in both nonirradiated and UVB-irradiated cells. These results demonstrated that CSE has not only strong protective effects against UVB-induced oxidative stress but also the regulatory effects on AP-1 activation.

A recent study of ours showed that immature aloe (baby aloe extract [BAE]) and aloesin, which is the main active component of BAE, had protective effects against UVB-induced skin photoaging in NHDFs. The expression of procollagen type I was 74% higher in UVB-irradiated cells treated with 25 μ g/mL BAE compared with untreated cells.²⁵ Moreover, another of our earlier studies demonstrated that royal jelly (RJ) and 10-hydroxy-2-decenoic acid protects against UVB damage in human fibroblasts. Treatment of UVB-irradiated cells with RJ at a low concentration of 1 μ g/mL increased procollagen type I production (up to 64.6%).²⁷ Here, we found that the inhibitory effect of CSE on UVB-induced skin photoaging was higher than that of BAE and RJ. UVB-exposed, CSE-treated cells (100 μ g/mL) had greater procollagen type I production (up to 266%) and less MMP-1 expression (up to 19%) than nontreated cells (Fig. 4). These results indicate that CSE may strongly protect against damage caused by UVB radiation. Since transforming growth factor-beta 1 (TGF- β 1) is well known to be the major regulator of procollagen type I synthesis, TGF- β 1 production in the CSE-treated NHDFs was determined.^{25,35} However, CSE did not influence secretion of TGF- β 1 (data not shown). We did not explore the mechanisms by which procollagen type I synthesis was increased in this study, so we will investigate the mechanisms of these effects of CSE in future studies.

In this study, we found evidence that CSE has a protective effect against UVB-induced skin photoaging in NHDFs. First, the UVB-induced attenuation of procollagen type I production was restored by CSE treatment (Fig. 4B). Second, the UVB-induced activation of MMP-1 in NHDFs was inhibited by CSE treatment (Fig. 4C). Third, the inhibitory effect of CSE on procollagen type I production and MMP-1 expression was dose dependent. Fourth, the UVB-induced phosphorylations of c-Jun and c-Fos were inhibited by CSE treatment.

Our results showed the regulatory effect of CSE on procollagen type I and MMP-1 production as well as AP-1 activation in normal NHDF cells without UVB irradiation. In addition, the effects of CSE on skin aging-related biomarkers are more potent in UVB-irradiated cells than in non-UVB-irradiated normal cells.

UV radiation causes skin changes such as increased wrinkles, roughness, a sallow appearance, mottled hyperpigmentation, and telangiectasias.³⁶ In an *in vivo* study of human skin, chronic UVB exposure was found to decrease the production of procollagen type I, leading to collagen loss and increased wrinkling, skin thickening, and reduced skin elasticity.^{28,37} Using histological techniques, we observed the changes associated with photoaging in hairless mice treated with CSE. Specifically, mice treated with CSE had thinner epidermal layers and denser collagen fibers compared with untreated mice (Fig. 6).

Inomata *et al.* reported that the activity of MMPs increases over wide areas of mouse skin during chronic UVB exposure, contributing to wrinkle formation through destruction of the basement membrane followed by degradation of ECM components, including collagen fibers.³⁸ However, mice treated with topical CSE had higher procollagen type I levels and lower MMP-1 levels than untreated mice. In this study, RP, which is the most commonly used retinyl ester in cosmetics,³⁹ was used as a positive control. Even the inhibitory effect of CSE on photoaging was found to be stronger than that of RP in the skin of hairless mice. Specifically, UVB-irradiated mice treated topically with 1% CSE had 18% more expression of procollagen type I compared with the RP-treated group. In other words, these findings have implications for the use of CS in that the substance may have use not only in an alternative cosmetic, but also in herbal medicine. CS has fatty acids such as oleic acid, linoleic acid, and palmitic acid, which have anti-inflammatory effects, potentiates wound healing, and is a moisturizer.^{40,41} Therefore, it is very useful as a cosmeceutical.

In conclusion, this study demonstrates that CSE significantly decreases UVB-induced MMP-1 expression and stimulates procollagen type I production by scavenging UVB-induced ROS in NHDFs *in vitro*. Furthermore, the *in vivo* results indicate that CSE prevents the degradation of collagen and elastin fiber by upregulating TGF- β 1 activity and downregulating MMP-1. This article is the first which demonstrates the ability of CS extract to protect the skin against photoaging. Although we used GC-MS analysis to determine the various fatty acids of CS leaves, including linolenic acid,²⁵ we did not isolate the active constituents that inhibit UVB-induced skin damage. Therefore, further research is warranted to identify the compounds responsible for these anti-photoaging effects.

ACKNOWLEDGMENTS

This work was supported by a grant from the “National Research Foundation of Korea (NRF-20100025362)” and the “Cooperative Research Program for Agriculture Science

& Technology Development (PJ0074792012),” Rural Development Administration, Republic of Korea.

AUTHOR DISCLOSURE STATEMENT

The authors declare that there are no conflicts of interest.

REFERENCES

- Gupta K, Thakral KK, Arora SK, Wagle DS: Studies on growth, structural carbohydrates and phytate in coriander (*Coriander sativum*) during seed development. *J Sci Food Agric* 1986;54: 43–46.
- Grieve M: *A Modern Herbal*, Vol. 1. (Leyel H, ed.) Dover Publications, New York, 1971.
- Bajpai M, Mishra A, Prakash D: Antioxidant and free radical scavenging activities of some leafy vegetables. *Int J Food Sci Nutr* 2005;56:73–81.
- Gray AM, Flatt PR: Insulin-releasing and insulin-like activity of the traditional anti-diabetic plant *Coriandrum sativum* (coriander). *Br J Nutr* 1999;81:203–209.
- Lal AA, Kumar T, Murthy PB, Pillai KS: Hypolipidemic effect of *Coriandrum sativum* L. in triton-induced hyperlipidemic rats. *Indian J Exp Biol* 2004;42:909–912.
- Sreelatha S, Padma PR, Umadevi M: Protective effects of *Coriandrum sativum* extracts on carbon tetrachloride-induced hepatotoxicity in rats. *Food Chem Toxicol* 2009;47:702–708.
- Cortes-Eslava J, Gomez-Arroyo S, Villalobos-Pietrini R, Espinosa-Aguirre JJ: Antimutagenicity of coriander (*Coriandrum sativum*) juice on the mutagenesis produced by plant metabolites of aromatic amines. *Toxicol Lett* 2004;153:283–292.
- Medhin DG, Hadhazy P, Bakos P, Verzar-Petri G: Hypotensive effects of *Lupinus termis* and *Coriandrum sativum* in anaesthetized rats. A preliminary study. *Acta Pharm Hung* 1986;56: 59–63.
- Al-Said MS, Al-Khamis KI, Islam MW, Parmar NS, Tariq M, Ageel AM: Post-coital antifertility activity of the seeds of *Coriandrum sativum* in rats. *J Ethnopharmacol* 1987;21:165–173.
- Wu TT, Tsai CW, Yao HT, *et al.*: Suppressive effects of extracts from the aerial part of *Coriandrum sativum* L. on LPS-induced inflammatory responses in murine RAW 264.7 macrophages. *J Sci Food Agric* 2010;90:1846–1854.
- Reuter J, Huyke C, Casetti F, *et al.*: Anti-inflammatory potential of a lipolotion containing coriander oil in the ultraviolet erythema test. *J Dtsch Dermatol Ges* 2008;6:847–851.
- Chithra V, Leelamma S: *Coriandrum sativum* changes the levels of lipid peroxides and activity of antioxidant enzymes in experimental animals. *Indian J Biochem Biophys* 1999;36: 59–61.
- Fisher GJ, Wang Z, Datta SC, Varani J, Kang S, Voorhees JJ: Pathophysiology of premature skin aging induced by ultraviolet light. *N Engl J Med* 1997;337:1419–1428.
- Rittié L, Fisher GJ: UV-light-induced signal cascades and skin aging. *Ageing Res Rev* 2002;1:705–720.
- Quan T, He T, Kang S, Voorhees JJ, Fisher GJ: Solar ultraviolet irradiation reduces collagen in photoaged human skin by blocking transforming growth factor-beta type II receptor/Smad signaling. *Am J Pathol* 2004;165:741–751.
- Vincenti MP, Brinckerhoff CE: Transcriptional regulation of collagenase (MMP-1, MMP-13) genes in arthritis Integration of

- complex signaling pathways for the recruitment of gene-specific transcription factors. *Arthritis Res* 2002;4:157–164.
17. Pilcher BK, Sudbeck BD, Dumin JA, Welgus HG, Parks WC: Collagenase-1 and collagen in epidermal repair. *Arch Dermatol Res* 1998;290:S37–S46.
 18. Varani J, Warner RL, Gharaee-Kermani M, *et al.*: Vitamin A antagonizes decreased cell growth and elevated collagen-degrading matrix metalloproteinases and stimulates collagen accumulation in naturally aged human skin. *J Invest Dermatol* 2000;114:480–486.
 19. Brenneisen P, Wenk J, Klotz LO, *et al.*: Central role of ferrous/ferric iron in the ultraviolet B irradiation-mediated signaling pathway leading to increased interstitial collagenase MMP-1 and stromelysin-1 MMP-3 mRNA levels in cultured human dermal fibroblasts. *J Biol Chem* 1998;273:5279–5287.
 20. Watanabe H, Shimizu T, Nishihira J, *et al.*: Ultraviolet A-induced production of matrix metalloproteinase-1 is mediated by macrophage migration inhibitory factor (MIF) in human dermal fibroblasts. *J Biol Chem* 2004;279:1676–1683.
 21. Quan T, He T, Voorhees JJ, Fisher GJ: Ultraviolet irradiation induces Smad7 via induction of transcription factor AP-1 in human skin fibroblasts. *J Biol Chem* 2005;280:8079–8085.
 22. Lam PY, Yan CW, Chiu PY, Leung HY, Ko KM: Schisandrin B protects against solar irradiation-induced oxidative stress in rat skin tissue. *Fitoterapia* 2011;82:393–400.
 23. Wlaschek M, Tantcheva-Poor I, Naderi L, *et al.*: Solar UV irradiation and dermal photoaging. *J Photochem Photobiol B* 2001;63:41–51.
 24. Demeule M, Brossard M, Pagé M, Gingras D, Béliveau R: Matrix metalloproteinase inhibition by green tea catechins. *Biochim Biophys Acta* 2000;1478:51–60.
 25. Park G, Kim HG, Kim YO, Park SH, Kim SY, Oh MS: *Coriandrum sativum* L. protects human keratinocytes from oxidative stress via regulating oxidative defense systems. *Skin Pharmacol Physiol* 2012;25:93–99.
 26. Hwang E, Kim SH, Lee S, *et al.*: A comparative study of baby aloe and adult aloe on UVB-induced skin photoaging: an *in vitro*. *Phytother Res* 2013;27:1874–1882.
 27. Park HM, Hwang E, Lee KG, Han SM, Cho Y, Kim SY: Royal jelly protects against ultraviolet B-induced photoaging in human skin fibroblasts via enhancing collagen production. *J Med Food* 2011;14:899–906.
 28. Kang TH, Park HM, Kim YB, *et al.*: Effects of red ginseng extract on UVB irradiation-induced skin aging in hairless mice. *J Ethnopharmacol* 2009;123:446–451.
 29. Chiu TM, Huang CC, Lin TJ, Fang JY, Wu NL, Hun CF: *In vitro* and *in vivo* anti-photoaging effects of an isoflavone extract from soybean cake. *J Ethnopharmacol* 2009;126:108–113.
 30. Cho JW, Cho SY, Lee SR, Lee KS: Onion extract and quercetin induce matrix metalloproteinase-1 *in vitro* and *in vivo*. *Int J Mol Med* 2010;20:347–352.
 31. Kehrer JP: Free radicals as mediators of tissue injury and disease. *CRC Crit Rev Toxicol* 1993;23:21–48.
 32. Aruoma OI: Nutrition and health aspects of free radicals and antioxidant. *Food Chem Toxicol* 1994;62:671–683.
 33. Nickavar B, Abolhasani FA: Screening of antioxidant properties of seven Umbelliferae fruits from Iran. *Pak J Pharm Sci* 2009;22:30–35.
 34. Satyanarayana S, Sushruta K, Sarma GS, Srinivas N, Subba Raju GV: Antioxidant activity of the aqueous extracts of spicy food additives—evaluation and comparison with ascorbic acid in *in-vitro* systems. *J Herb Pharmacother* 2004;4:1–10.
 35. Choi MS, Yoo MS, Son DJ, *et al.*: Increase of collagen synthesis by obovatol through stimulation of the TGF-beta signaling and inhibition of matrix metalloproteinase in UVB-irradiated human fibroblast. *J Dermatol Sci* 2007;46:127–137.
 36. Bernstein EF, Uitto J: The effect of photodamage on dermal extracellular matrix. *Clin Dermatol* 1996;14:143–151.
 37. Hwang E, Sun Z, Lee TH, *et al.*: Enzyme-processed Korean Red Ginseng extracts protects against skin damage induced by UVB irradiation in hairless mice. *J Ginseng Res* 2013;37:425–434.
 38. Inomata S, Matsunaga Y, Amano S, *et al.*: Possible involvement of gelatinases in basement membrane damage and wrinkle formation in chronically ultraviolet B-exposed hairless mouse. *J Invest Dermatol* 2003;120:128–134.
 39. FDA Center for Food Safety and Applied Nutrition: Voluntary Cosmetics Registration Program. 2004. www.cfsan.fda.gov/_dms/cos-regn.html (accessed September 2006).
 40. Rodrigues HG, Vinolo MA, Magdalon J, *et al.*: Oral administration of oleic or linoleic acid accelerates the inflammatory phase of wound healing. *J Invest Dermatol* 2012;132:208–215.
 41. Garidel P, Fölting B, Schaller I, Kerth A: The microstructure of the stratum corneum lipid barrier: mid-infrared spectroscopic studies of hydrated ceramide:palmitic acid:cholesterol model systems. *Biophys Chem* 2010;150:144–156.